Int J Clin Exp Med 2018;11(12):13259-13266
www.ijcem.com /ISSN:1940-5901/IJCEM0085748

Original Article

Apoptosis induced by endoplasmic reticulum stress is involved in the lungs of hyperoxia-induced bronchopulmonary dysplasia rats

Kehuan Wang*, Lanlan Mi*, Ting Zhang, Huimin Ju, Ming Chang, Hongyan Lu

*Department of Pediatrics, The Affiliated Hospital of Jiangsu University, Zhenjiang 212001, China. *Equal contributors.*

Received September 19, 2018; Accepted November 8, 2018; Epub December 15, 2018; Published December 30, 2018

Abstract: The pathogenesis of bronchopulmonary dysplasia (BPD) is currently undefined, however apoptosis induced by endoplasmic reticulum (ER) stress is considered as a key mechanism. The present study was performed in a BPD rat model to determine the role of ER stress-induced apoptosis. In total, 48 preterm Sprague-Dawley rats were randomly divided into two groups that included the BPD group and the control group. The rats in the BPD group were continually exposed to 85% hyperoxia, during the time that the rats in the control group were exposed to room air. Eight rats in each group were euthanized at 7, 14, and 21 days after exposure. Alveolarization was assessed by performing radial alveolar counts (RAC). Apoptosis in lung cells was evaluated by TdT-mediated dUTP nick end labeling (TUNEL). Real-time quantitative RT-PCR and Western blot were used to detect pulmonary expression of ER chaperone 78-kDa glucose-regulated/binding immunoglobulin protein (GRP78), ER stress-associated apoptosis proteins c-jun-N-terminal kinase (JNK), C/EBP-homologous protein (CHOP) and the caspase-12. Compared with the control group, hyperoxia exposure resulted in lower RAC and significant apoptosis. Furthermore, BPD rats were found to have increased mRNA and protein expression of GRP78, caspase-12, CHOP, and JNK. These data demonstrate that ER stress-induced apoptosis is involved in the pathogenesis of BPD.

Keywords: Bronchopulmonary dysplasia, endoplasmic reticulum stress, apoptosis, rat

Introduction

Infants born very prematurely are at substantial risk for the development of bronchopulmonary dysplasia (BPD) after supplemental oxygen therapy [1]. Although the exact mechanisms by which hyperoxia causes lung injury are incompletely understood, both generation of ROS and cellular apoptosis appear to play important roles. ROS can induce apoptosis through either intrinsic or extrinsic apoptosis pathways [2]. Much evidence has indicated that endoplasmic reticulum (ER) stress is associated with apoptosis. In mammalian cells, the ER is an important organelle with functions of maintaining intracellular calcium homeostasis, protein secretion, lipid synthesis, protein glycosylation, and folding [3]. Interruption of ER homeostasis causes ER stress and triggers the unfolded protein response (UPR), which can lead to apoptosis in persistently stressed cells. The 78-kDa glucose-regulated/binding immunoglobulin protein (GRP78) is a hallmark for both the UPR and ER stress responses [4], and it responds rapidly to ER stress to enhance cell survival. However, if protein aggregation is persistent and the stress cannot be resolved, signaling switches from pro-survival to pro-apoptotic ER stress response [5-7]. Compelling evidence suggests that caspase-12 in rodents (caspase-4 in humans), C/EBP-homologous protein (CHOP), and c-jun-N-terminal kinase (JNK) are recruited to participate in ER stress-induced apoptosis. Furthermore, a growing body of evidence suggests that oxidative stress-induced ER stress may be crucial in the regulation of apoptotic cell death. However, the importance of ER stress and the role of ER stress-induced apoptotic cell death in the pathogenesis of neonatal lung injury and BPD are unknown.

Table 1. The sequence for each primer and product length

	Sequence (5'-3')	Length (bp)
GRP78	F: CCGTAACAATCAAGGTCTACGA	124
	R: AAGGTGACTTCAATCTGGGGTA	
Caspase-12	F: TCCTGGTCTTTATGTCCC	180
	R: CGATAGCCCAAGGAAGTG	
CHOP	F: CCAGCAGAGGTCACAAGCAC	126
	R: CGCACTGACCACTCTGTTTC	
JNK	F: TGATGACGCCTTACGTGGTA	114
	R: GGCAAACCATTTCTCCCATA	
β-actin	F: GCAGAAGGAGATTACTGCCCT	136
	R: GCTGATCCACATCTGCTGGAA	

The primers' sequence and product length designed for GRP78, caspase-12, CHOP, JNK and β-actin.

Material and methods

Animal model

All animal procedures were approved by the Animal Care and Ethics Committee of Jiang Su University [8]. A newborn rat model of BPD established by our research group as previously described was used. In total, 21 females (200-220 g) and seven males (220-250 g) Sprague-Dawley rats (Experimental Animal Center of Jiang Su University, Zhenjiang, China) were left overnight for mating in groups of four consisting of three females and one male. The day on which the vaginal plug was identified was considered to be the first day of pregnancy. On the 21st day of pregnancy (term =22 days), the pregnant rats were anesthetized with intraperitoneal injections of 10% chloral hydrate (350 mg/kg; Wuhan Boster Biological Technology, Wuhan, China), and then underwent delivery via uterine-incision, resulting in pups deemed premature.

Within 24 hours of birth, 48 newborn rats were randomly divided into BPD group and control group (n=24, each). The rats in the BPD group were exposed to 85% hyperoxia, monitored continuously by an oxygen analyzer (model 572; Servomex Co., Inc., Norwood, MA, USA), while the rats in the control group were exposed to room air (21% oxygen). All other conditions and control factors were the same. The nursing rats were exchanged between the 2 groups every 24 hours to avoid oxygen toxicity.

Lung histology and morphometric analysis

At 7, 14, and 21 days after the start of exposure to hyperoxia or room air, eight rats from both groups were randomly selected and sacrificed with intraperitoneal injections of 10% chloral hydrate. Whole lungs were collected aseptically by chest opening. The left lungs were fixed in 4% paraformaldehyde for hematoxylin-eosin (HE) staining and terminal deoxynucleotidyl transferase-mediated dUTP nick end labeling (TUNEL) assay, while the right lobes of the lungs were used for mRNA detection and Western blot analysis. The left lobes of the lungs were fixed in 4% paraformaldehyde overnight and embedded in paraffin. The paraffin-embedded sections (4-μm-thick) were stained with H&E. Morphological changes were evaluated using an optical microscope. Alveolarization was assessed by performing radial alveolar count (RAC), according to the method of Emery and Mithal [9]. From the center of the respiratory bronchiole, a perpendicular was drawn to the edge of the acinus, defined by a connective tissue septum or the pleura, and the number of septa intersected by this line was counted. A total of ten counts were performed for each animal.

TUNEL assay

A TUNEL assay was performed to detect apoptotic cell in lung sections. TUNEL staining using the TUNEL detection kit (Roche Diagnostics, Mannheim, Germany) was carried out according to the manufacturer's instruction. Images of cells taken using Olympus BX51 microscope at a magnification of 400X. Sections incubated with PBS, instead of TDT enzyme solution served as negative controls. The TUNEL-positive cells were counted in five randomly selected visual fields. Apoptosis index (AI) was represented as the ratio of apoptosis.

Real-time quantitative RT-PCR

Total RNA was extracted from the tissue samples by the Trizol reagent (Invitrogen, Carlsbad, CA, USA). The concentration of total RNA was quantified using spectrophotometry (Bio-Rad Laboratories, Hercules, CA, USA). Then, 1 μg of total RNA was reverse transcribed using the Prime Script RT reagent kit from TaKaRa (TaKaRa, Japan). Quantitative RT-PCR was per-

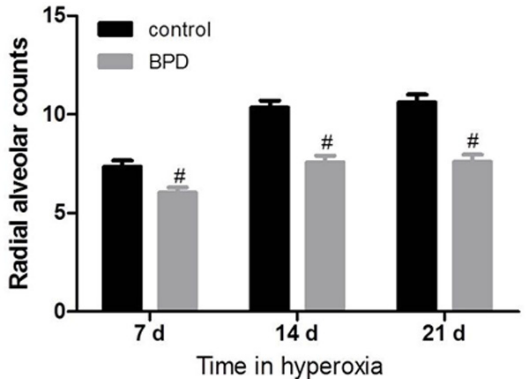

Figure 1. Effects of hyperoxia on lung histology and RAC. Compared with control rats, the lung histology of the rats exposed to hyperoxia was characterized by simpler alveolar structure, fewer and larger alveoli. The lung histology of the neonatal rats exposed to hyperoxia also exhibited a pattern of alveolar simplification in the 14 and 21-day-old rats. The alveolar number determined by the RAC was reduced after hyperoxic exposure. Data are expressed as the mean ± standard deviation. $^{\#}P<0.01$, compared with the control. RAC, radial alveolar counts.

formed using the Agilent Stratagene Mx3000P Real-Time QPCR System (Agilent, USA) with SYBR *Premix Ex Taq*™ reagent kit (TaKaRa, Japan). The oligonucleotide primers and products were shown in **Table 1**. PCR conditions were: denaturation at 95°C for 30 sec; amplification at 95°C (5 sec) and 60°C (30 sec) for 40 cycles. Relative mRNA levels of target genes were determined by comparing with standard curves and normalization to β-actin. Each reaction was amplified in triplicate and ratio results were calculated based on the $2^{-\Delta CT}$ method [10].

Western blot analysis

Total protein was extracted from the tissue samples, the content of which was measured by plotting a standard curve with the BCA method. Then, the protein was separated by sodium dodecyl sulfate polyacrylamide gel electrophoresis (SDS-PAGE) and transferred to a polyvinylidene difluoride (PVDF) membrane. After blocking with 5% nonfat dry milk, the membranes were incubated overnight at 4°C with the following primary polyclonal rabbit anti-rat antibodies: GRP78, caspase-12, CHOP, p-JNK (1:500; Abcam, Cambridge, UK). Following washing three times in Tris-buffered saline with 0.1% Tween 20 (TBST) for 10 minutes, the membranes were incubated with horseradish peroxidase-labeled goat anti-rabbit IgG antibody (1:5000; Wuhan Boster Biological Technology, Wuhan, China) at room temperature for 2 hours.

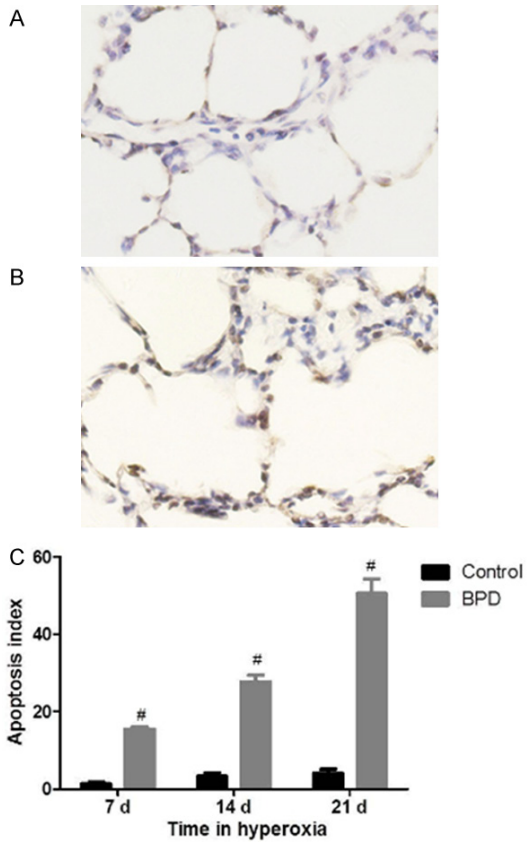

Figure 2. A, B. TUNEL staining demonstrates a significant increase in TUNEL-positive cells, in a pattern similar to that observed by immunohistochemical staining at 14 days (magnification, x400). A. Control group; B. BPD group. More epithelial and endothelial cells were apoptotic in the BPD group than in the control group. C. The apoptosis index was increased gradually over the duration of hyperoxic exposure, and the percentages of apoptotic cells were significantly higher, compared with the control groups. Data are expressed as the mean ± standard deviation. $^{\#}P<0.01$, compared with the control. TUNEL, TdT-mediated dUTP nick end labeling.

The target proteins were detected by the enhanced chemiluminescence system (Applygen Technologies, Beijing, China). The membranes were then exposed to X-ray film, fixed, scanned and quantified using a GDS-800 Complete Gel Documentation & Analysis system (Microtek Lab, Carson, CA, USA). β-actin was used as the internal reference. Relative protein expression level was represented by the ratio of gray value of the target protein to that of the internal reference protein.

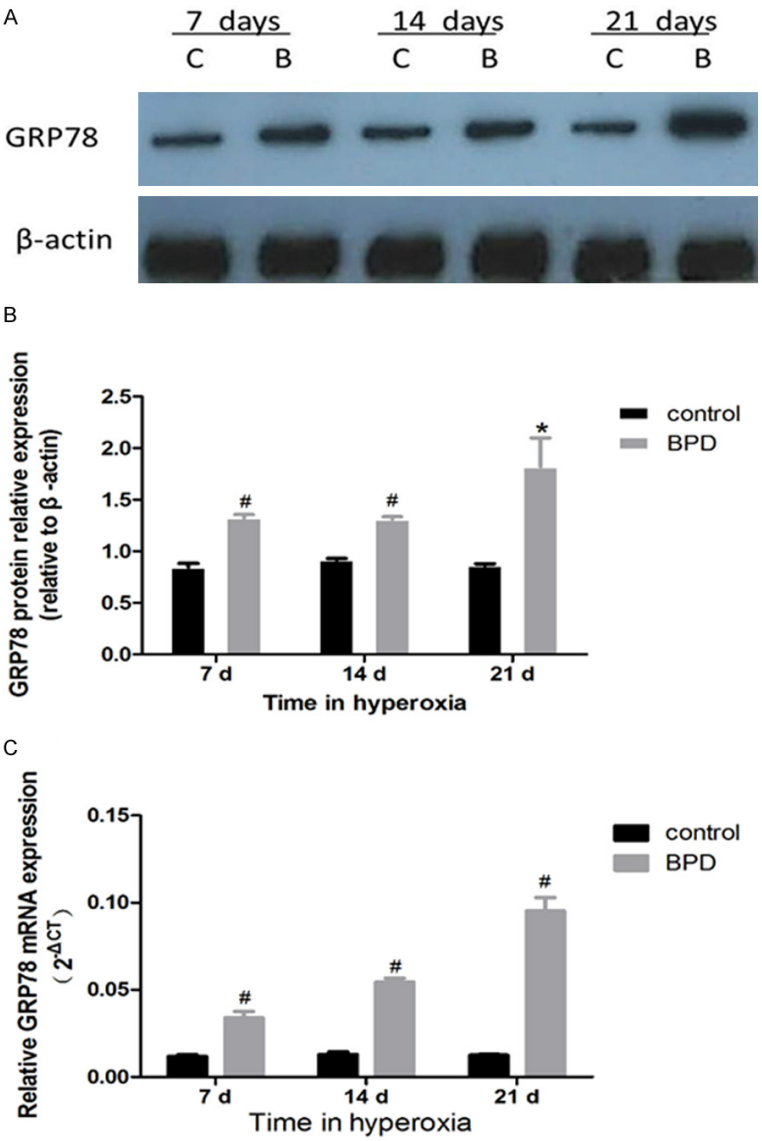

Figure 3. GRP78 protein and mRNA levels in lung tissues following hyperoxia. In the BPD groups, GRP78 protein, as determined by Western blot (A and B) and mRNA, as determined by real-time quantitative RT-PCR (C), were highly expressed in lung tissues after 7 days of hyperoxia, and increased gradually between 7 and 21 days. Data are expressed as the mean ± standard deviation. #P<0.01, *P<0.05, compared with the control. GRP78, 78-kDa glucose-regulated/binding immunoglobulin protein. C: Control group, B: BPD group.

Statistical analysis

All data are presented as mean ± standard deviation. SPSS17.0 software (SPSS, Chicago, IL, USA) was used for statistical analysis. Inter-group comparisons conforming to normal distribution were made using two independent sample t-tests, and multiple group comparisons made using one-way analysis of variance (ANOVA). P<0.05 was considered to indicate a statistically significant.

Results

Lung histology and RAC

The lungs exposed to air room gradually mature as the time, showing structured alveolar structure, more uniform size alveoli and thinner alveolar septa. However, the alveolarization of the lungs exposed to hyperoxia was impaired. Compared with the control groups, the lung histology of the rats exposed to hyperoxia was characterized by simpler alveolar structure, having fewer and larger alveoli. These alterations in the lungs are consistent with the hallmark features of BPD [11]. RAC was performed to quantify the apparent decreases in the number of alveoli. As shown in **Figure 1**, the RAC values in the BPD groups were significantly decreased than those in the control groups (P<0.01) at the same time-points.

Localization of apoptosis and AI

There were a few TUNEL-positive cells in the control groups, while numerous positive cells in the BPD groups at all-time points. The TUNEL-positive cells in the BPD groups were preferentially located in the alveoli, small airway epithelial cells and vascular endothelial cells (**Figure 2A**, **2B**). Compared with the control groups at the same time-points, the AI values in the BPD groups were all significantly increased (P<0.01), and that the AI values in the BPD groups increased with extension of the duration of hyperoxic exposure (**Figure 2C**).

GRP78 expression levels in lung tissues

GRP78, one important molecular chaperone localized in ER, has been extensively consid-

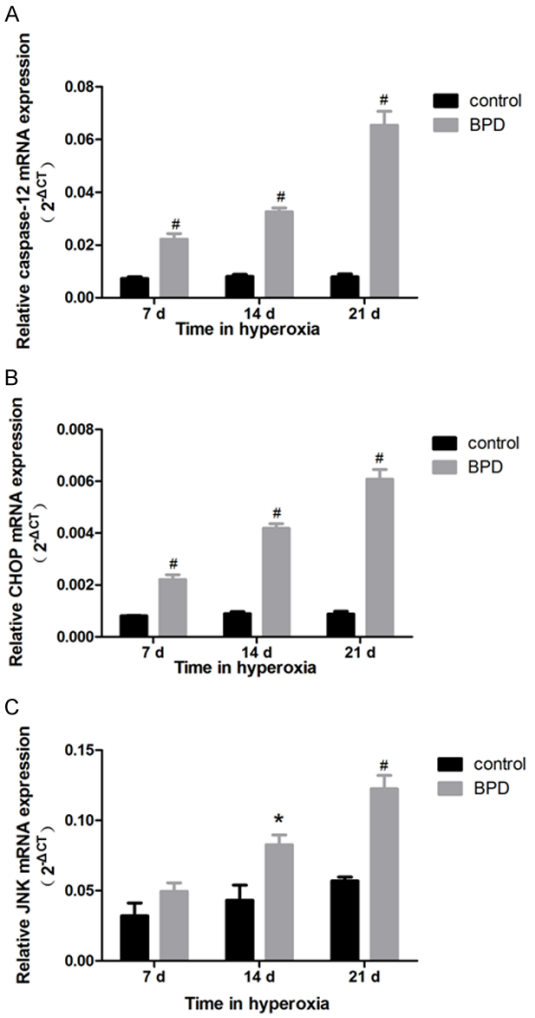

Figure 4. mRNA levels of caspase-12, CHOP, and JNK, determined using real-time quantitative RT-PCR. Following hyperoxia, the mRNA levels of caspase-12 and CHOP increased gradually between 7 and 21 days, and the levels were significantly higher, compared with the control groups (A and B). JNK mRNA were equally expressed in the BPD groups after 7 days of hyperoxia compared to the control groups and were highly expressed after 14 and 21 days (C). Data are expressed as the mean ± standard deviation. $^{\#}P<0.01$, $^{*}P<0.05$, compared with the control. CHOP, C/EBP-homologous protein; JNK, c-jun-N-terminal kinase.

ered as an important indicator for the induction of ER stress. As shown in **Figure 3**, the mRNA and protein expression levels of GRP78 in the BPD groups were significantly increased more than those in the control groups on postnatal days 7, 14, and 21 ($P<0.05$ at all-time points). The up-regulated expression of GRP78 indicated the activation of ER stress.

Expression of ER stress-associated apoptotic factors in lung tissues

Caspase-12, CHOP, and JNK are the key apoptotic factors in the three branches of ER stress-associated apoptosis pathways. To determine whether hyperoxia induced ER stress-associated apoptosis, real-time quantitative RT-PCR and Western blot analysis were performed to detect the expression levels of ER stress-associated apoptotic factors, including caspase-12, CHOP, and JNK, in lung tissues exposed to hyperoxia and room air. The mRNA expression levels of caspase-12 and CHOP increased gradually over 7, 14, and 21 days, and the expression levels were significantly higher than those in the control groups (**Figure 4A**, **4B**). The increased differences between the two groups became more significant as the duration of hyperoxia exposure. JNK mRNA was equally expressed in the BPD groups after 7 days of hyperoxia compared to the control groups and were highly expressed after 14 and 21 days (**Figure 4C**). Furthermore, Western blot analysis showed the same trends of caspase-12, CHOP, and pho-JNK at the protein expression levels, as shown in **Figure 5**. These data demonstrated that ER stress-associated apoptotic factors are activated in the hyperoxia-exposed newborn rat lungs, further supporting the hypothesis that hyperoxia induced ER stress-associated apoptosis is involved in the pathogenesis of BPD.

Discussion

Bronchopulmonary dysplasia (BPD) is a multifactorial disease that remains the most serious lung condition of prematurity, and a significant cause of mortality in preterm infants. Over the past few decades, the incidence of BPD has significantly raised as a result of improved survival of smaller and more immature infants requiring mechanical ventilation [12].

Acute and chronic lung injury and impaired postnatal lung growth are thought to be responsible for the pathogenesis of BPD [13]. Oxygen toxicity caused by mechanical ventilation and oxygen therapy is considered to be one of the major contributing factors [1, 14]. In this study, it was demonstrated that prolonged exposure to hyperoxia disrupted postnatal alveolarization and led to the development of BPD in rats.

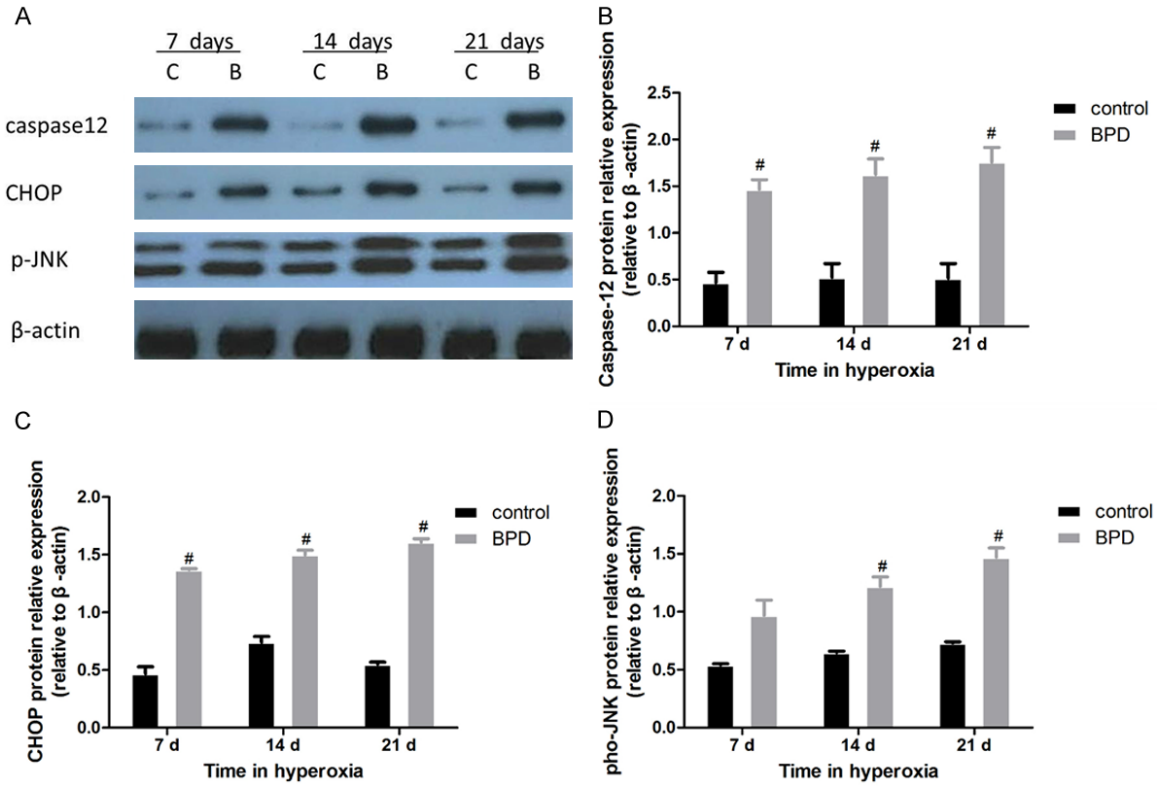

Figure 5. Protein levels of caspase-12, CHOP, and phospho-JNK, determined using Western blot analysis. Following hyperoxia, the protein levels of caspase-12, CHOP and JNK increased gradually between 7 and 21 days (A). The protein levels of caspase-12 and CHOP were significantly higher after 7 days of hyperoxia, compared with the control groups (B and C). Phospho-JNK protein was significantly higher after 14 days of hyperoxia (D). Data are expressed as the mean ± standard deviation. $^{\#}P<0.01$, $^{*}P<0.05$, compared with the control. CHOP, C/EBP-homologous protein; JNK, c-jun-N-terminal kinase. C: control group, B: BPD group.

Although the exact mechanisms are incompletely understood, both generation of ROS and cellular apoptosis appear to play important roles.

Recent studies have shown that ROS produced during supplemental oxygen therapy can induce apoptosis in the lungs of premature rats [15]. Consistent with these studies, this study showed that a higher proportion of epithelial and endothelial cells were apoptotic in the BPD groups, compared with the control groups.

There is mounting evidence demonstrating that ER stress implicate in apoptosis and play an important role in the development of various lung diseases, including chronic obstructive pulmonary disease [16], interstitial lung disease [17] and lung cancer [18]. The involvement of ER stress and ER stress-induced apoptosis in the pathophysiology of BPD is a relatively new area of research.

Thus, we examined the expression of GRP78, caspase-12, CHOP, and JNK in lung cells of a hyperoxia-induced preterm newborn rat BPD model to investigate this relation.

GRP78 is a central regulator of ER homeostasis and is involved in activation of the ER stress response. Under normal conditions, GRP78 binds to the transmembrane ER stress sensors to form an inactive complex. During the ER stress response, these transmembrane sensors dissociate from GRP78 and trigger subsequent signaling pathways to induce apoptosis [19]. In this study, expression of GRP78 in the BPD groups increased with extension of the duration of hyperoxic exposure and the expression levels were significantly higher than those in the control groups, which indicated the activation of ER stress.

Three apoptosis pathways are known to be involved in the ER stress-induced apoptosis.

There are the caspase-12 dependent pathway, transcriptional induction of CHOP, and activation of the JNK dependent pathway [20, 21]. The caspase family plays an important role in regulating apoptosis [3]. Caspase-12, an ER-resident caspase, is cleaved and activated specifically during ER stress. Cleaved caspase-12 will trigger the activation of caspase-9, followed by activation of caspase-3, and finally, trigger apoptosis [22, 23]. Upregulation of caspase-12 only occurs during ER stress [24]. Therefore, we used caspase-12 as the key mediators of ER stress-induced apoptosis. In this study, the protein and mRNA expression of caspase-12 were increased in the BPD groups when compared with the control groups, which indicated activation of ER stress-induced apoptosis. CHOP is the first identified protein that mediates ER stress-induced apoptosis and much is known on the roles of this molecule in apoptosis [25]. Increased expression of CHOP has previously been reported in the lung epithelial cell of mouse exposed to hyperoxia [26]. Consistent with the previous report, increased apoptosis and higher expression levels of CHOP in the BPD rats was detected and a positive correlation was found with persistent hyperoxic exposure. Furthermore, hyperoxia increased JNK expression after 14 and 21 days.

In conclusion, this study clearly demonstrates that exposure to 85% hyperoxia induces expression of caspase-12, CHOP, and JNK in preterm rats. Thus, activation of ER stress-induced apoptosis is involved in the pathogenesis of BPD. These novel findings may provide a treatment of BPD through targeting inhibition of lung ER stress.

Acknowledgements

This work was financially supported by the National Natural Science Foundation of China (No.81741052, 81370746).

Disclosure of conflict of interest

None.

Address correspondence to: Hongyan Lu, Department of Pediatrics, The Affiliated Hospital of Jiangsu University, Zhenjiang 212001, China. Tel: 86-158-62979315; E-mail: lhy5154@163.com

References

[1] Amata E, Pittalà V, Marrazzo A, Parenti C, Prezzavento O, Arena E, Nabavi SM, Salerno L. Role of the Nrf2/HO-1 axis in bronchopulmonary dysplasia and hyperoxic lung injuries. Clin Sci (Lond) 2017; 131: 1701-1712.

[2] Xu D, Perez RE, Rezaiekhaligh MH, Bourdi M, Truog WE. Knockdown of ERp57 increases BiP/GRP78 induction and protects against hyperoxia and tunicamycin-induced apoptosis. Am J Physiol Lung Cell Mol Physiol 2009; 297: 44-51.

[3] Yan M, Chen K, He L, Li S, Huang D, Li J. Uric acid induces cardiomyocyte apoptosis via activation of calpain-1 and endoplasmic reticulum stress. Cell Physiol Biochem 2018; 45: 2122-2135.

[4] Ruggiero C, Doghman-Bouguerra M, Ronco C, Benhida R, Rocchi S, Lalli E. The GRP78/BiP inhibitor HA15 synergizes with mitotane action against adrenocortical carcinoma cells through activation of ER stress pathways. Mol Cell Endocrinol 2018; 474: 57-64.

[5] Malhotra JD, Kaufman RJ. The endoplasmic reticulum and the unfolded protein response. Semin Cell Dev Biol 2007; 18: 716-731.

[6] Lai E, Teodoro T, Volchuk A. Endoplasmic reticulum stress: signaling the unfolded protein response. Physiology (Bethesda) 2007; 22: 193-201.

[7] Zhang K, Kaufman RJ. Signaling the unfolded protein response from the endoplasmic reticulum. J Biol Chem 2004; 279: 25935-25938.

[8] Lu HY, Zhang J, Wang QX, Tang W, Zhang LJ. Activation of the endoplasmic reticulum stress pathway involving CHOP in the lungs of rats with hyperoxia-induced bronchopulmonary dysplasia. Mol Med Rep 2015; 12: 4494-5000.

[9] Sallon C, Soulet D, Tremblay Y. Morphometry of pulmonary tissue: from manual to high throughput automation. Rev Mal Respir 2017; 34: 1072-1084.

[10] Noorbazargan H, Nadji SA, Samiee SM, Paryan M, Mohammadi-Yeganeh S. New design, development, and optimization of an in-house quantitative TaqMan real-time PCR assay for HIV-1 viral load measurement. HIV Clin Trials 2018; 23: 1-8.

[11] O'Reilly M, Thébaud B. Animal models of bronchopulmonary dysplasia. The term rat models. Am J Physiol Lung Cell Mol Physiol 2014; 307: 948-958.

[12] Rivera L, Siddaiah R, Oji-Mmuo C, Silveyra GR, Silveyra P. Biomarkers for bronchopulmonary dysplasia in the preterm infant. Front Pediatr 2016; 4: 33.

[13] Gien J, Kinsella JP. Pathogenesis and treatment of bronchopulmonary dysplasia. Current Opinion in Pediatrics 2011; 23: 305-313.
[14] Saugstad OD. Oxygen and oxidative stress in bronchopulmonary dysplasia. J Perinat Med 2010; 38: 571-577.
[15] Hattori Y, Kotani T, Tsuda H, Mano Y, Tu L, Li H, Hirako S, Ushida T, Imai K, Nakano T, Sato Y, Miki R, Sumigama S, Iwase A, Toyokuni S, Kikkawa F. Maternal molecular hydrogen treatment attenuates lipopolysaccharide-induced rat fetal lung injury. Free Radic Res 2015; 49: 1026-37.
[16] Somborac-Bacura A, van der Toorn M, Franciosi L, Slebos DJ, Zanic-Grubisic T, Bischoff R, van Oosterhout AJ. Cigarette smoke induces endoplasmie reticulum stress response and proteasomal dysfunction in human alveolar epithelial cells. Exp Physiol 2013; 98: 316-325.
[17] Kropski JA, Lawson WE, Young LR, Blackwell TS. Genetic studies provide clues on the pathogenesis of idiopathic pulmonary fibrosis. Dis Model Mech 2013; 6: 9-17.
[18] Hsin IL, Hsiao YC, Wu MF, Jan MS, Tang SC, Lin YW, Hsu CP, Ko JL. Lipocalin 2, a new GADD153 target gene, as an apoptosis inducer of endoplasmic reticulum stress in lung cancer cells. Toxicol Appl Pharmacol 2012; 263: 330-337.
[19] Park KW, Eun Kim G, Morales R, Moda F, Moreno-Gonzalez I, Concha-Marambio L, Lee AS, Hetz C, Soto C. The endoplasmic reticulum chaperone GRP78/BiP modulates prion propagation in vitro and in vivo. Sci Rep 2017; 7: 44723.
[20] Yao W, Yang X, Zhu J, Gao B, Shi H, Xu L. IRE1α siRNA relieves endoplasmic reticulum stress-induced apoptosis and alleviates diabetic peripheral neuropathy in vivo and in vitro. Sci Rep 2018; 8: 2579.
[21] Arshad M, Ye Z, Gu X, Wong CK, Liu Y, Li D, Zhou L, Zhang Y, Bay WP, Yu VC, Li P. RNF13, a RING finger protein, mediates endoplasmic reticulum stress-induced apoptosis through the inositol-requiring enzyme (IRE1α)/c-Jun NH2-terminal kinase pathway. J Biol Chem 2013; 288: 8726-36.
[22] Yan Z, He JL, Guo L, Zhang HJ, Zhang SL, Zhang J, Wen YJ, Cao CZ, Wang J, Wang J, Zhang MS, Liang F. Activation of caspase-12 at early stage contributes to cardiomyocyte apoptosis in trauma-induced secondary cardiac injury. Sheng Li Xue Bao 2017; 69: 367-377.
[23] Chinta SJ, Rane A, Poksay KS, Bredesen DE, Andersen JK, Rao RV. Coupling endoplasmic reticulum stress to the cell death program in dopaminergic cells: effect of paraquat. Neuromolecular Med 2008; 10: 333-42.
[24] Bernales S, Papa FR, Walter P. Intracellular signaling by the unfolded protein response. Annu Rev Cell Dev Biol 2006; 22: 487-508.
[25] Grechowa I, Horke S, Wallrath A, Vahl CF, Dorweiler B. Human neutrophil elastase induces endothelial cell apoptosis by activating the PERK-CHOP branch of the unfolded protein response. FASEB J 2017; 31: 3868-3881.
[26] Lozon TI, Eastman AJ, Matute-Bello G, Chen P, Hallstrand TS, Altemeier WA. PKR-dependent CHOP induction limits hyperoxia-induced lung injury. Am J Physiol Lung Cell Mol Physiol 2011; 300: 422-429.